Elastic-Plastic Analysis of the PVRC Burst Disk Tests With Comparison to the ASME Code Primary Stress Limits

D. P. Jones
Mem. ASME

J. E. Holliday

Bechtel Bettis, Inc.,
Bettis Atomic Power Laboratory,
West Mifflin, PA 15122-0079

This paper provides a comparison between finite element analysis results and test data from the Pressure Vessel Research Council (PVRC) burst disk program. Testing sponsored by the PVRC over 20 yr ago was done by pressurizing circular flat disks made from three different materials until failure by bursting. The purpose of this reanalysis is to investigate the use of finite element analysis (FEA) to assess the primary stress limits of the ASME Boiler and Pressure Vessel Code (hereafter the Code), and to qualify the use of elastic-plastic (EP-FEA) for limit-load calculations. The three materials tested represent the range of strength and ductility found in modern pressure vessel construction and include a low-strength, high-ductility material, a medium-strength, medium-ductility material, and a high-strength, low-ductility, low-alloy material. Results of elastic and EP-FEA are compared to test data. Stresses from the elastic analyses are linearized for comparison of Code primary stress limits to test results. Elastic-plastic analyses are done using both best-estimate and elastic-perfectly plastic (EPP) stress-strain curves. Both large strain-large displacement (LSLD) and small strain-small displacement (SSSD) assumptions are used with the EP-FEA. Analysis results are compared to test results to evaluate the various analysis methods, models, and assumptions as applied to the bursting of thin disks. The test results show that low-strength, high-ductility materials have a higher burst capacity than do high-strength, low-ductility materials. Linearized elastic FEA stresses and ASME Code primary stress limits provide excessive margins to failure for the burst disks for all three materials. The results of these studies show that LSLD EP-FEA can provide a best-estimate analysis of the disks, but the accuracy depends on the material stress-strain curve. This work concludes that SSSD EPP analysis methods provide a robust and viable alternative to the current elastic linearization method of satisfying the primary stress limits of the Code. [S0094-9930(00)01602-4]

Introduction

The PVRC Subcommittee on effective utilization of yield strength conducted burst tests on disk specimens of a number of different steels to study the effect of yield stress on failure. The program considered the influence of yield strength, as related to strain-hardening exponent or to yield-to-tensile strength ratio, upon the bursting pressure of components containing strain-concentrating geometries. Cooper et al. [1] reported the results of these tests and the results were further used by Langer [2].

The disks were analyzed by Riccardella [3] using an elastic-plastic discrete shell element program. The disks are reanalyzed here using continuum elements since these are more commonly used today in pressure vessel and piping analyses. Comparing FE analysis results is of interest to provide qualification of finite element computer programs that are used to compute limit load solutions for use in assessing primary stress limits of the ASME Code [4]. In this paper, three of the tests conducted by the PVRC were selected to compare the test results to analysis results. Each disk was analyzed three ways: a standard ASME Code primary stress evaluation using elastic analysis, EP-FEA using strain-hardening characteristics of the material, and EPP-FEA to compute a limit load for the disks.

The burst disks were 152-mm-dia flat circular plates 3 mm thick. The disks were clamped in a test fixture and hydrostatically pressurized to bursting. Three materials were used to make the plates: a low-strength, high-ductility stainless steel; a medium-strength, medium-ductility carbon steel; and high-strength, low-ductility, low-alloy steel. Records of transverse deflection versus pressure and burst pressure were recorded for each test.

In this paper, results from the tests are compared to results from FEA made using various assumptions of elastic-plastic material properties and strain-displacement relationships. Results from the analyses are used to assess the various assumptions relative to the test data. Linearized elastic stresses are used for comparison with ASME Code primary stress limits and these results are compared to the burst pressures for each test. Finally, observed burst pressures are compared to limit-load solutions obtained by using EPP-FEA.

Testing

A detailed summary of the test phase of this investigation is discussed in the forthcoming. Testing was sponsored by the PVRC and completed over 20 yr ago [1].

The test specimens were hydrostatically pressure tested to bursting in a test fixture, as shown schematically in Fig. 1. Pressure was increased from zero until the disks failed by catastrophic bursting. The tests were all performed at room temperature.

The specimens tested by PVRC consisted of three 152-mm-dia circular plates 3 mm thick. The geometry associated with the specimens is shown in Fig. 2.

The materials of the three specimens tested are 304 stainless

Contributed by the Pressure Vessels and Piping Division and presented at the Pressure Vessels and Piping Conference, Boston, Massachusetts, August 1–5, 1999, of THE AMERICAN SOCIETY OF MECHANICAL ENGINEERS. Manuscript received by the PVP Division, January 6, 2000; revised manuscript received March 7, 2000. Technical Editor: S. Y. Zamrik.

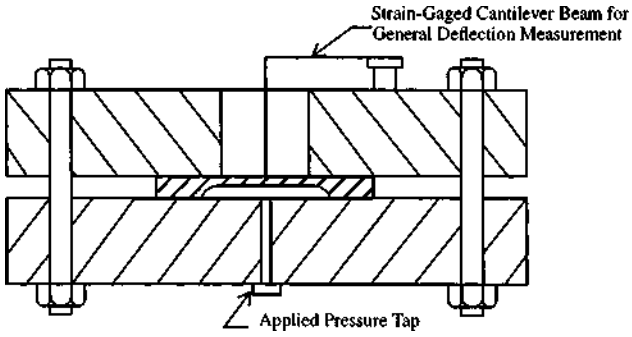

Fig. 1 PVRC test fixture

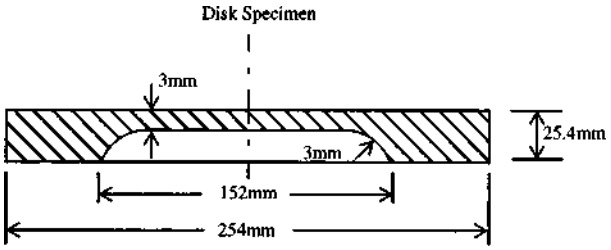

Fig. 2 Disk specimen

Table 1 Material properties

Material	Yield Strength MPa	Ultimate Strength MPa	Uniform Strain	Reduction of Area
304 SS	234	579	0.54	0.74
ABS-C	269	440	0.31	0.66
A-533-B	510	662	0.17	0.68

steel (304 SS), ABS-C carbon steel, and A533 Grade B low-alloy steel (A-533-B). Material properties associated with these materials are shown in Table 1.

Test Results

Central deflection was measured with a cantilever beam device. Central deflection versus pressure data along with maximum burst pressure and failure location were provided in [1]. The central deflection versus pressure records on each specimen are given in Figs. 10–12. In interests of safety, deflection measurements were stopped after about 50 mm of deflection. The disks were then pressurized until failure.

Burst pressure and failure location for each disk are as follows:

- 304 SS burst disk, 6800 psi (46.9 MPa)—failure at the center of the disk by ductile rupture.
- ABS-C burst disk, 3750 psi (25.9 MPa)—failure at the center of the disk by ductile rupture.
- A-533-B burst disk, 5300 psi (36.5 MPa)—failure at the built in edge of the plate by cracking.

Analysis

The following FE analyses were conducted in this study:

- Elastic FEA of the burst disks including linearization of the elastic FEA results per Code methods.
- LSLD EP-FEA of the burst disks using a bilinear true stress-true plastic strain curve.

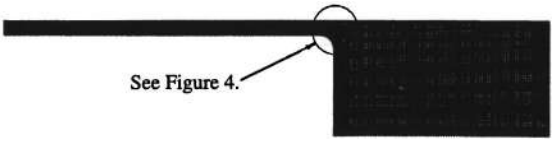

Fig. 3 Finite element model

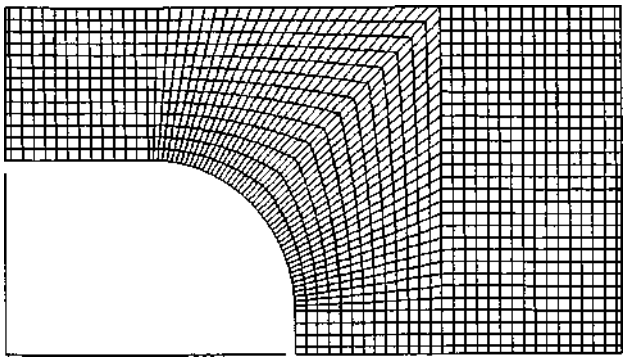

Fig. 4 Close-up of built-in edge

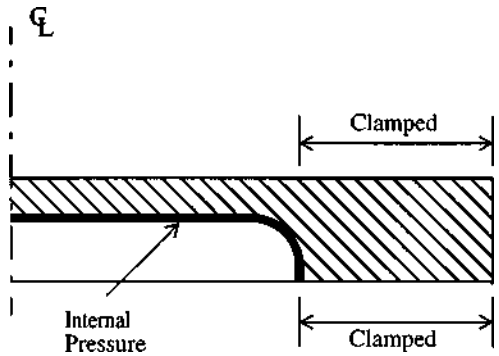

Fig. 5 Boundary conditions for FEA models

- SSSD EPP-FEA of the burst disks using $1.5S_m$ as the limit load input strength parameter for the analysis. S_L is used as a yield strength in the EPP-FEA analysis.
- The elastic FEA was conducted using an in house FEA program. The in-house program and ABAQUS give identical results for elastic problems.
- Stress linearization of the elastic FEA result was conducted using standard stress linearization routines consistent with the recommendations of the PVRC study by Hechmer and Hollinger [5].
- The EP and EPP finite element analyses were conducted using the ABAQUS [6] program and the FEA model generated using PATRAN [7].

The finite element model used to conduct the elastic, the LSLD EP and SSSD EPP FEAs of the test specimen is a two-dimensional (2-D) axisymetric model and is shown in Fig. 3. An enlargement of the built-in section showing the mesh around the fillet is shown in Fig. 4. The finite element model consists of:

- 23,966 eight-node reduced integration quadrilateral elements (ABAQUS element CAX8R)
- 73,151 nodes

Boundary conditions applied to the FE model are shown in Fig. 5. The clamped in portion of the specimen is assumed to be fixed

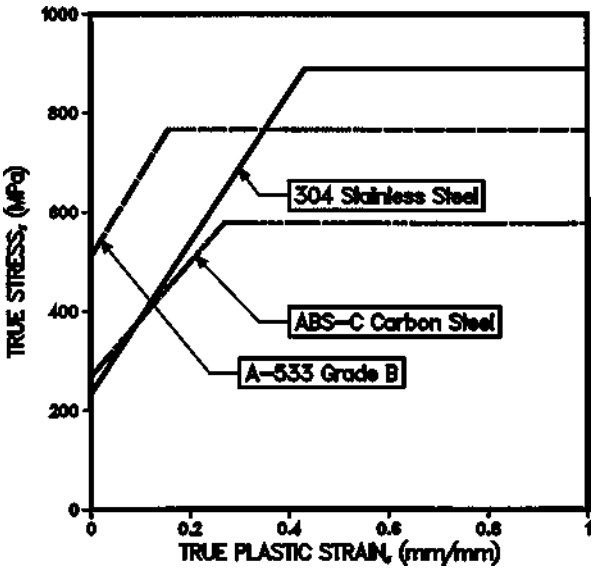

Fig. 6 True stress versus true plastic strain curve

Table 2 True-stress, true-strain values

Material	Yield Strength S_y, MPa	Engineering Ultimate S_{ult}, MPa	True Ultimate Strength MPa	True Uniform Strain
304 SS	234	579	892	0.432
ABS-C	269	440	576	0.270
A-533-B	510	662	774	0.157

Table 3 Material allowable strength

Material	$2S_y/3$ MPa	$S_{ult}/3$ MPa	S_m MPa
304 SS	156	193	156
ABS-C	179	147	147
A-533-B	340	221	221

against all motion. There was no motion of these surfaces observed during the test. A symmetry boundary condition was used at the center of the models.

Both the elastic and EP analyses used Young's modulus of 206×10^3 MPa and Poisson's ratio of 0.3. A bilinear true-stress, true-strain curve was used for the LSLD EP and the SSSD EPP analyses. These curves are shown in Fig. 6. Tabular values are given in Table 2. ASME sets allowable strength (S_m) as the lower of $2S_y/3$ or $S_{ult}/3$. Table 3 provides this assessment for the three materials.

Yield Criterion. The elastic-plastic analyses are conducted assuming von Mises yield criterion and an isotropic-hardening material law. Isotopic hardening is considered reasonable since the specimens were tested by application of monotonically increasing pressure to failure, with no reversal of load. Thus, cyclic hardening concerns are limited to very local unloading regions and considered second order for these tests.

Failure Definition. The LSLD and SSSD EP-FEA are carried out until the numerical solutions becomes unstable, e.g., when a converged solution for an additional increment of load is numerically difficult to obtain. At this point, the slope of the pressure-deflection curve for the disks becomes vanishingly small. The total pressure that causes this condition is the incipient failure pressure.

Failure in the tests was defined when the disks burst. Instead of trying to predict local rupture, tearing, or cracking from the FEA results, it is proposed here that a useful definition of failure is the pressure for which the structure approaches dimensional instability, i.e., unbounded deflection for a small increment in pressure. This condition is symptomatic of an ill-conditioned boundary value problem caused by the combined changes in geometry and material stiffness leading to a physical instability. This is often preceded by numerical convergence problems. The numerical convergence problem is indicative of impending structural collapse and is characterized by the slope of the load-deflection approaching zero. A horizontal load-deflection plot means that the deflection grows unbounded with a small increase in load.

Comparisons

Analysis results are compared to appropriate test data in this section.

Elastic FEA Results. The FEA stress results were linearized to compute membrane plus bending stress intensity for comparison to Code primary membrane plus bending stress intensity allowables. The linearization cut lines (called stress classification lines or SCLs by Hechmer and Hollinger [5]) are shown in Fig. 7. Linearizations were made at a total of 642 SCLs in the burst disk. This number of SCLs was used to enable a clear understanding of the distribution of $[P_m+P_b]/p$ and does not imply that this many SCLs are required for design evaluations. A plot of normalized membrane plus bending stress intensity divided by applied pressure versus cut line is shown in Fig. 7. The worst case membrane plus bending stress intensity occurs at SCL 587, which is 9 deg beyond the point of tangency of the 3-mm fillet. This location is at the built-in edge where the bending moment due to the pressure is large. Since this moment is not needed for static equilibrium, it is a redundant moment and not required in a primary stress evalua-

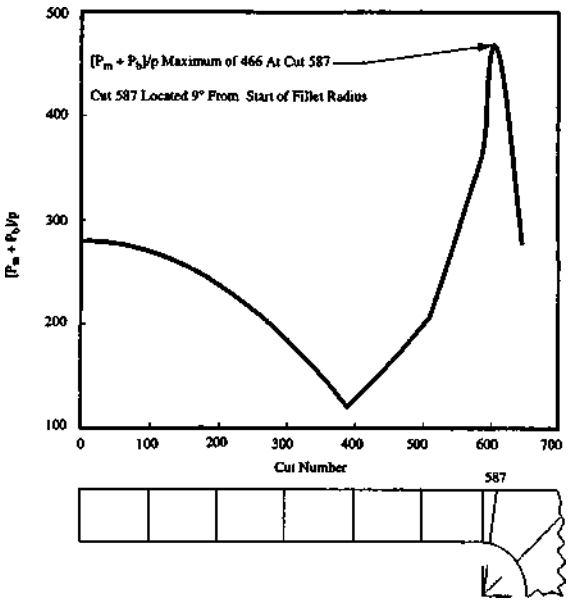

Fig. 7 Linearized elastic stresses

Table 4 Linearization results

Material	Allowable Pressure	Worst Case Location
304 SS	73 psi (0.503 MPa)	Built in edge (SCL 587)
ABS-C	69 psi (0.473 MPa)	Built in edge (SCL 587)
A-533-B	103 psi (0.710 MPa)	Built in edge (SCL 587)

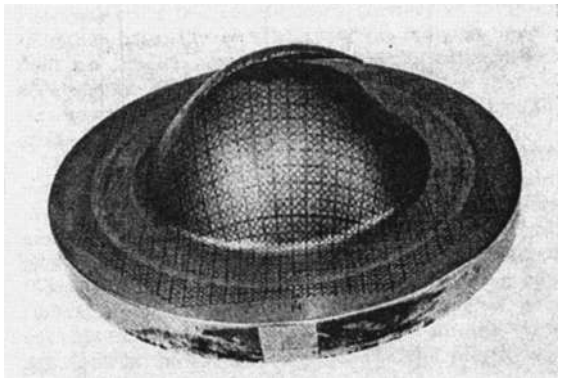

Fig. 8 Centerline failure

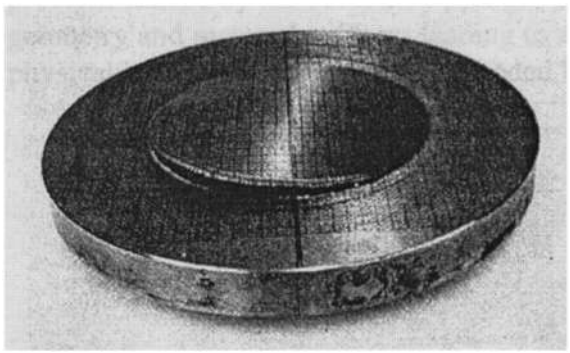

Fig. 9 A-533-B edge failure

tion in the Code. However, an elastic FEA analyzes does not provide enough information by itself to determine whether or not a linearized stress is primary or secondary.

From Fig. 7, it is observed that the largest linearized stress is equal to 466*p*. Dividing this result into the 1.5 S_m from Table 3 for the three materials gives the elastic based allowable pressures for three burst disks given in Table 4. The elastic results predict that the limiting location is always at the built-in edge of the plate, suggesting that the plates should all fail at this location regardless of material. Test results, however, show that the ductile 304 SS and ABS-C disks fail in the center, while the A-533-B less ductile plate fails at the built-in edge. Test failure locations are easily observed from the photographs in [1] repeated here in Figs. 8 and 9. For this geometry, the largest $[P_m+P_b]/p$ location can be used to predict the location of the failure only for the A-533-B material.

EP-FEA Results. A comparison between test and LSLD EP-FEA results for applied pressure versus maximum centerline deflection response is provided in Figs. 10–12. From these figures, it is observed that LSLD EP-FEA predicts the essential character of

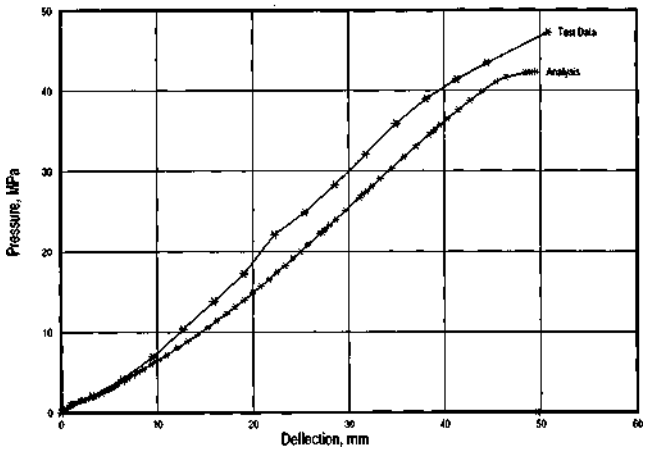

Fig. 10 Pressure-deflection curve for 304 SS.LSLD-EP-FEA

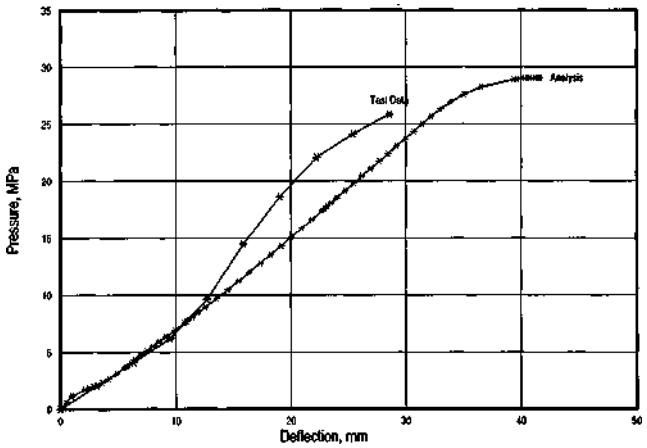

Fig. 11 Pressure-defection curve for ABS-C.LSLS-EP-FEA

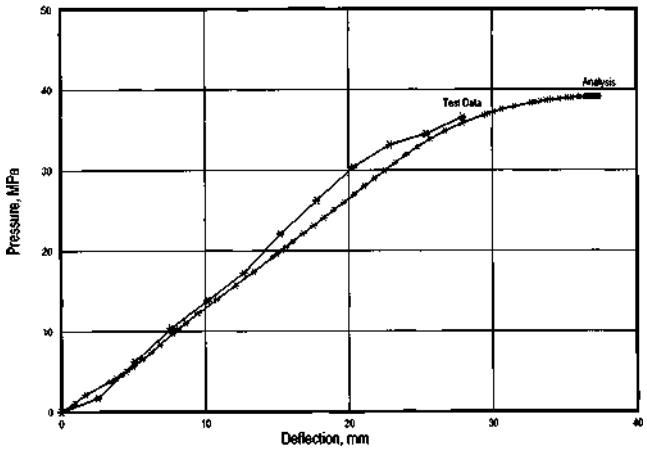

Fig. 12 Pressure-deflection curve for A-533-B.LSLD-EP-FEA

the pressure deflection response of the specimens. The analytical results are considered to agree well with the test data, especially in view of the simplified stress-strain curves used to characterize the material behavior of the three materials tested and evaluated. Since the available stress-strain data for the actual materials is very limited, bilinear true stress-true plastic strain curves shown in Fig. 6 are used in the LSLD EP-FEA.

Table 5 Burst pressure comparisons

Material	LSLD EP-FEA Analysis Result	Test Result
304 SS	6,138 psi (42.3 MPa)	6,800 psi (46.9 MPa)
ABS-C	4,214 psi (29.1 MPa)	3750 psi (25.9 MPa)
A-533-B	5,675 psi (39.1 MPa)	5300 psi (36.5MPa)

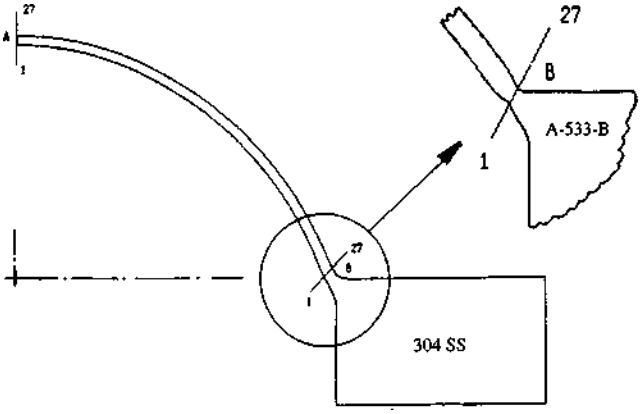

Fig. 13 Deformed geometry and cut line definitions

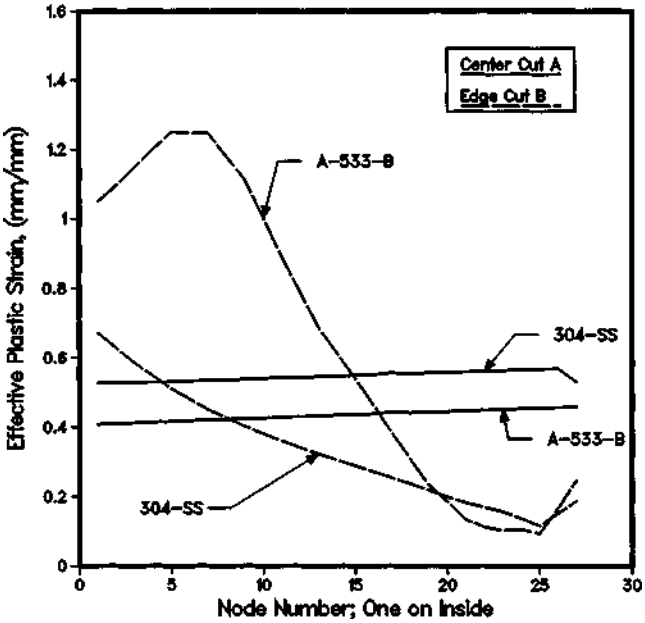

Fig. 14 Effective plastic strain distributions

A power-law representation was tried as suggested by Updike and Kalnins [8], and the predicted failure pressures were not significantly changed. Since actual material stress-strain curves are not available, there is no clear way to improve the material model at this point.

Burst pressures are obtained from the LSLD EP-FEA by finding the pressure for which a small increase in pressure results in a very large increase in deflection are compared to observed test burst pressures in Table 5.

Table 6 Limit load solutions

Material	LL Strength Parameter	Limit Load
304 SS	1.5 S_m = 34,000 psi (234 MPa)	204 psi (1.41 MPa)
ABS-C	1.5 S_m = 32,000 psi (221 MPa)	192 psi (1.32 MPa)
A-533-B	1.5 S_m = 48,000 psi (331 MPa)	299 psi (2.06 MPa)

It is observed from Fig. 8 that the low-strength, high-ductility 304 SS disk failed at the center of the disk by ductile rupture. The same is true for the ABS-C disk. Figure 9 shows that the high-strength, low-ductility A-533-B burst disk failed at the built-in edge of the disk because the material does not possess sufficient ductility to permit the development of the strains necessary for the disk to deform to the point where failure in the membrane could occur.

Figure 13 shows the deformation plot for the largest converged load step for the 304 SS disk from the LSLD EP-FEA. The insert on that figure allows comparisons with the deformation at the built in edge found for the A-533-B disk.

Figure 14 shows distributions of equivalent plastic strain (PEEQ) along cut line A and B for the 304 SS and A-533-B disks for the largest converged load step. The deformation plot and PEEQ plot for the ABS-C disk is about the same as for the 304 SS disks. The largest PEEQ peak is at the built in edge for all three disks. However, the largest through-thickness average PEEQ is at the center of the 304 SS and ABS-C disks and at the built in edge for the A-533-B disk. These observations support the notion that the actual failure site may be predicted by finding the location of the highest through-thickness average PEEQ.

EPP-FEA Results. Limit load (LL) can be calculated using SSSD EPP FEA programs. The pressure for the last converged solution from a SSSD EPP FEA problem is taken as an estimate of the LL. The results of these computations are given in Table 6. It is observed that the LL is proportional to the LL strength parameter, selected for this evaluation to equal $1.5S_m$. From Table 6, it is observed that even though the 304 SS has the lowest yield strength, it has a higher LL strength parameter, and therefore a higher LL, than the ABS-C burst disk. The LL for the A-533-B is the greatest of all three specimens reflecting its higher strength.

Discussion of Results

Calculated burst pressure are compared with test data for each of the specimens for the linearized elastic stress analysis results, the SSSD EPP LL results, and the LSLD EP results in Table 7.

Table 7 Ratio of test over predicted burst pressure

Material	Burst pressure, test	Elastic Linearized	SSSD EPP	LSLD EP
304 SS	6800 psi (46.9 MPa)	93	33	1.11
ABS-C	3750 psi (25.9 MPa)	54	20	0.89
A-533-B	53-0 psi (36.5 MPa)	51	18	0.93

Table 7 gives the ratio of measured burst pressure divided by the calculated burst pressure for each disk.

From Table 7, it is seen that linearized elastic FEA results provide the largest margins to failure, while limit analysis provides substantially lower, but adequate, margins to failure. LSLD EP-FEA provides a best-estimate analysis of burst pressure. However, it should also be noted that the EPP analyses are limited by S_{ult} because the slope assumed for the bilinear stress-strain curve is set by the uniform elongation strain.

The large failure margins associated with linearized elastic stress analysis are due primarily to the fact that the limiting location for that stress in the burst disk occurs near the built in edge and includes a significant contribution to from the redundant bending moment. The stress from a redundant moment may be secondary if equilibrium can be maintained in the absence of the moment. This is one of the major difficulties associated with using linearized elastic FEA to satisfy the primary stress limits of the Code. It is very difficult to differentiate primary from secondary stresses in redundant structures such as this one. As a result, secondary stresses are commonly included in the Code primary stress evaluations. While this is always conservative, it can result in designs that are excessively thick.

SSSD EPP limit analysis results provide significantly reduced failure margins compared to linearized elastic results because at the limit load, by definition, only primary stresses exist in the structure. Thus, the plate is permitted to carry higher pressure, and therefore have a reduced failure margin. However the reduced failure margins do not compromise the structural integrity of the plate since the margins are in excess of the minimum required margin to burst failure of 3.0 required by the Code. The reason that the SSSD EPP LL failure margins are still in excess of 3.0 is twofold: 1) the analysis does not account for increase in structural strength due to strain hardening, and 2) the analysis does not account for geometric strengthening as the plate deforms into a spherical shape. Geometric strengthening is quite large for thin flat plates because they deform to nearly a sphere before rupture. Other initial geometries may not experience such large geometric strengthening.

The failure margins associated with the LSLD EP-FEA results are considered best-estimate and only as accurate as the stress-strain curve used in the analysis. The approximate bilinear stress-strain curve used here produced -9.7 to 12.3 percent error relative to the measured test burst pressures. Improved stress-strain curves should enable improved estimates. Power-law models were used but since the data is not available to provide a credible power-law model, results are not reported here.

Observations

The following observations are made as a result of this work:

1 Burst pressures predicted for flat rupture disks by comparing linearized elastic FEA stress results to ASME Code primary stress limits are well below actual measured burst pressures.

2 LSLD EP-FEA can be used to provide reasonable best-estimates of burst pressures. The accuracy of these predictions will depend on the accuracy of the material stress-strain curves.

3 SSSD EPP FEA provides a conservative estimate of burst pressure.

4 The failures observed in these tests are located at sites of large through-thickness averaged equivalent plastic strain calculated by LSLD EP-FEA.

Conclusions

These observations lead to the conclusion that small strain small deflection elastic perfectly plastic FEA satisfies the intent of the ASME Code primary stress limits because as the limiting load is approached, only primary stresses exist in the structure. Using small strain small deflection elastic perfectly plastic FEA as a method to compute the limit load for a structure is thus a conservative alternative way to evaluate the ASME Code primary stress limits.

Acknowledgments

The analysis presented here was performed under a U.S. Department of Energy contract with Bechtel Bettis, Inc. The authors acknowledge the many fruitful discussions with Bettis colleagues Dr. D. N. Hutula and Dr. J. L. Gordon regarding this topic. Dr. Jones also acknowledges the contributions of the ASME Subgroup on Design Analysis members particularly Mr. Stephen Adams, Professor A. Kalnins, and Mr. John Hechmer in providing many of the ideas that have found their way into this work. Mr. Holliday acknowledges his mother, Mrs. H. T. Holliday for the love, support and encouragement she gave to him during her life.

Nomenclature

P_m = primary membrane stress intensity, MPa (ksi)
$P_m + P_b$ = primary membrane plus bending stress intensity, MPa (ksi)
S_y = yield strength, MPa (ksi)
S_{ult} = ultimate strength, MPa (ksi)
S_m = material strength allowable, MPa (ksi)
S_L = limit-load input strength, MPa (ksi)
p = pressure, MPa (ksi)
FEA = finite element analysis
Code = ASME Boiler & Pressure Vessel Code
PVRC = Pressure Vessel Research Council
LL = limit load
LSLD = large strain, large deflection
SSSD = small strain, small deflection
EP = elastic plastic
EPP = elastic-perfectly plastic

References

[1] Cooper, W. E., Kottcamp, E. H., and Spiering, G. A., 1971, ''Experimental Effort on Bursting of Constrained Disks as Related to the Effective Utilization of Yield Strength,'' ASME Paper 71-PVP-49.
[2] Langer, B. F., 1971, ''Design-Stress Basis for Pressure Vessels'' (The William M. Murray Lecture, 1970), Experimental Mechanics, Jan.
[3] Riccardella, 1973, ''Elasto-Plastic Analysis of Constrained Disk Burst Tests,'' ASME J. Eng. Ind., Feb., pp. 129–136.
[4] The American Society of Mechanical Engineers Boiler and Pressure Vessel Code, 1998 Edition, New York, NY.
[5] Hechmer, J. L., and Hollinger, G. L., 1998, ''3-D Stress Criteria: Guidelines for Application,'' WRC Bulletin No. 429, Feb.
[6] ABAQUS, 1994, Hibbitt, Karlson and Sorenson, Inc., Version 5.4.
[7] PATRAN, 1990, PDA Engineering, Release 2.5, Oct.
[8] Updike, D. P., and Kalnins, A., 1996, ''Tensile Instability of Axisymetric Pressure Vessels,'' ASME 1996 Pressure Vessels and Piping Conference, PVP-Vol. 338, pp. 257–263.